

# AN ADVANCED SENSOR MODEL FOR PANORAMIC CAMERAS

Jafar Amiri Parian, Armin Gruen

Institute of Geodesy and Photogrammetry  
Swiss Federal Institute of Technology (ETH) Zurich  
(parian, agruen)@geod.baug.ethz.ch

Commission V, WG V/1

**KEY WORDS:** Close Range, Photogrammetry, Panoramic Camera, Calibration, Sensor, Modeling, Accuracy, Test

## ABSTRACT:

Digital terrestrial panoramic cameras constitute an interesting new development, which is currently primarily used for purely imaging purposes such as indoor imaging, landscape recording, tourism advertising and Internet representations. However, the capability of taking high-resolution images continuously over the full horizon generates an efficient means for 3D object reconstruction as well. For that the particular sensor model has to be established and the inherent accuracy potential has to be investigated. We designed a sensor model, which models substantial deviations from the pinhole model using additional parameters. The sensor model maps the object space into the image space. The mapping function is the pinhole model-based perspective transformation in the form of bundle equations. In practice, there are many systematic errors disturbing the ideal model, which can be modeled as additional parameters. Additional parameters relate to the camera itself, the configuration of camera and turntable, and mechanical errors of the camera system during rotation (i.e. tumbling). In this paper we will present the results of calibration with additional parameters for two panoramic cameras, which indicate a subpixel accuracy level for such highly dynamic systems. We also investigate into the problem of temporal stability of the systematic errors. Finally we will demonstrate the systems' accuracy in 3D point positioning, including minimal number of control points adjustment. With these new panoramic imaging devices we do have additional powerful sensors for image recording and efficient 3D object modeling.

## 1. INTRODUCTION

The first panoramic cameras used in Photogrammetry were film-based aerial cameras. The Manual of Photogrammetry, 1980 lists a number of types, which differ mechanically and optically from each other. A prototype of an aerial panoramic camera can be modeled as a camera with a cylindrical focal surface, in which the image is acquired by sweeping a slit across this surface (Hartley, 1993). Through the integration of CCD technology, new types of airborne and terrestrial digital panoramic cameras were generated, using Linear Array CCDs as imaging devices. The EYESCAN, jointly developed by German Aerospace Center (DLR) and KST Dresden GmbH and the SpheroCam, SpheronVR AG are two different types of line-based panoramic cameras. The EYESCAN camera as used in terrestrial photogrammetric applications was addressed in Scheibe et al., 2001. Schneider and Maas, 2003 and Amiri Parian and Gruen, 2003 have worked on the mathematical modeling of line-based panoramic cameras. Schneider and Maas investigated a geometrical model for a prototype of the EYESCAN panoramic camera and they performed calibration by using a 3D testfield (Schneider and Maas, 2003). They also performed 3D positioning using bundle block adjustment (Schneider and Maas, 2004). We have worked on the mathematical model of general line-based panoramic cameras. We performed calibration and accuracy test using a 3D testfield for EYESCAN and SpheroCam (Amiri Parian and Gruen, 2003). We improved mathematical model by modeling the mechanical error of the rotating turntable, tumbling, and we reported the improvement of the accuracy by a factor of two in the case of using tumbling parameters in the bundle adjustment process (Amiri Parian and Gruen, 2004).

In this paper, by defining image- and block-invariant parameters we put emphasis on 3D positioning using a minimal number of control points. The paper will be organized as follows. Chapter 1 gives a short review of the panoramic cameras SpheroCam and EYESCAN. Chapter 2 addresses our mathematical sensor model. Chapter 4 covers the result of adjustment, included the results of the physical measurement of the tumbling for the SpheroCam, and the calibration results of EYESCAN with/without tumbling parameters. In this chapter we demonstrate the system accuracy for EYESCAN using a testfield with as few as possible control points.

## 2. PANORAMA TECHNIQUES

Several techniques have been used for panoramic imaging. Mosaicing/stitching of a rotated frame-CCD camera, mirror technology including single mirror and multi mirrors, near 180 degrees with large frame cameras or one shot with fish-eye lens and recently a new technology of creating high resolution panoramic image by rotating a line-CCD camera are some known methods for panoramic imaging. Up to now, these techniques have mainly been used for pure imaging purposes, such as indoor imaging, landscape and cultural heritage recording, tourism advertising and image-based rendering, and recently for efficient Internet representations. Among the mentioned techniques for panoramic imaging, the last one has a possibility to produce a high-resolution panoramic image (more than 300 Mpixels) in one shot. The camera principle consists of a linear array, which is mounted on a high precision turntable parallel to the rotation axis. By rotation of the turntable, the linear array sensor captures the scenery as a continuous set of vertical scan lines.

Table 1. Parameters of EYESCAN and SpheroCam panoramic cameras

Parameters	EYESCAN	SpheroCam
Number of pixel in linear array (vertical format)	3600 or 10200 pixels per line	5300 pixels per line
Horizontal format (depends on the focal lens)	27489 pixels (35 mm lens)	39267 pixels (50 mm lens)
Pixel size	7 or 8 microns	8 microns

In our tests we used two line-based rotating panoramic cameras, a prototype of EYESCAN M3, a joint development between German Aerospace Center (DLR) and KST Dresden GmbH\*. The camera is engineered for rugged everyday field use as well as for the measurement laboratory. The other panoramic camera used here is the SpheroCam from the SpheronVR AG\*\* which operates similar to EYESCAN.

### 2.1. EYESCAN M3

Figure 1 shows the sensor system and Table 1 shows format parameters of the camera. The camera system contains three parts: camera head, optical part, and high precision turntable with a DC-gearsystem motor. The camera head is connected to the PC with a bi-directional fiber link for data transmission and camera control. The optical part of the system uses high performance Rhodenstock lenses. With adjustment rings one can use other lenses. The camera head is mounted on a high precision turntable with a sinus-commutated DC-gearsystem motor (Scheibe et al., 2001), internal motion control and direct controlling by the PC. Rotation speed and scan angle are pre-selectable and correspond to the shutter speed, image size and focal length of the lens. For a more detailed description see Schneider and Maas (2003).

### 2.2. SpheroCam

The structure of the SpheroCam (Figure 1) includes three parts, the camera head, the optical part which is compatible with NIKON-lenses, and a DC motor to rotate the Linear Array. The SpheroCam is specially designed for use with a fish-eye lens, with a near 180° vertical field of view. As it rotates about its vertical axis, the SpheroCam then captures a complete spherical image. It is designed to capture high quality images. Table 1 contains the format parameters of SpheroCam. For more detail on specifications of the camera see Amiri Parian and Gruen (2003).

## 3. SENSOR MODEL

The sensor model as a mapping function is based on a projective transformation in the form of bundle equations, which maps the 3D object space information into the 2D image space. The sensor model uses the following coordinate systems:

- Pixel coordinate system
- Linear Array coordinate system
- 3D auxiliary coordinate system
- 3D object coordinate system

Figure 2 shows the pixel coordinate (i, j) system. The original image observations are saved in this system. Figure 3 shows the other coordinate systems: Linear Array (0, y, z), auxiliary (X', Y', Z') and object space (X, Y, Z) coordinate systems. The



Figure 1. Digital terrestrial panoramic cameras. EYESCAN (left) and SpheroCam (right).

effects of lens distortion and the shift of the principal point are modeled in the Linear Array coordinate system. The rotation of the Linear Array and mechanical errors of the rotating turntable are modeled in the auxiliary coordinate system. The object space coordinate system is used as a reference for determining the exterior orientation parameters of the sensor.

To define the auxiliary coordinate system, an ideal panoramic camera is considered. Here the origin of the auxiliary coordinate system coincides with the projection center O. The rotation axis passes through the projection center and coincides with Z'. X' passes through the start position of the Linear Array before rotation and Y' is defined to get a right-handed coordinate system.

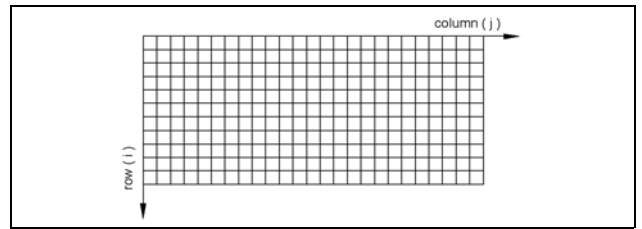


Figure 2. Pixel coordinate system (i, j).

The model, which directly relates pixel observations (i, j) to the object points (X, Y, Z), for an ideal sensor becomes (Amiri Parian and Gruen, 2003):

$$\begin{pmatrix} 0 \\ y \\ -c \end{pmatrix} = \lambda P^{-1} R_z^t(j A_h) M_{w,\varphi,k} \begin{pmatrix} X - X_o \\ Y - Y_o \\ Z - Z_o \end{pmatrix} \quad (1)$$

With

$$P = \begin{pmatrix} 0 & 0 & -1 \\ -1 & 0 & 0 \\ 0 & 1 & 0 \end{pmatrix} \quad y = (i - \frac{N}{2}) A_v$$

Where,  $A_h$  is horizontal pixel size and  $A_v$  is vertical pixel size. N is the number of pixel in linear array.

\* <http://www.kst-dresden.de/>

\*\* <http://www.spheron.com/>

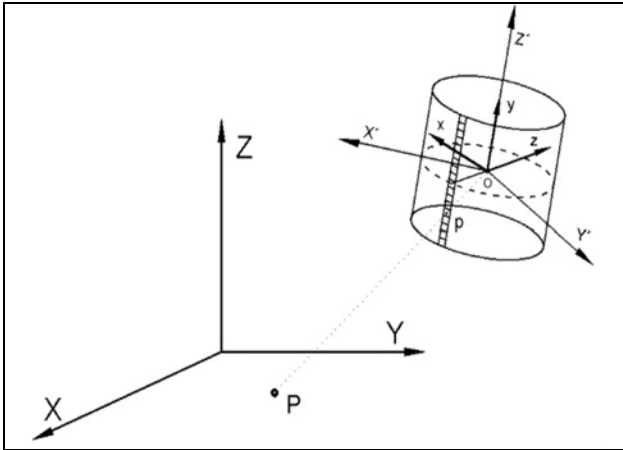


Figure 3. Object coordinate ( $X, Y, Z$ ), auxiliary coordinate ( $X', Y', Z'$ ) and Linear Array ( $0, y, z$ ) coordinate systems.

There are many systematic errors disturbing the ideal sensor model. The most important ones, with a distinct physical meaning, are:

- 1) Radial lens distortion (2 parameters)
- 2) Shift of principal point (1 parameter)
- 3) Camera constant (1 parameter)
- 4) Tilt and inclination of the Linear Array with respect to the rotation axis (2 parameters)
- 5) Eccentricity of the projection center from the origin of the auxiliary coordinate system (2 parameters)
- 6) Resolution of rotation (1 parameter)
- 7) Tumbling (3 or 6 parameters)

The above errors are modeled as additional parameters for a prototype of a panoramic camera. The results of the modeling for two different cameras were reported in Amiri Parian and Gruen (2003, 2004).

The additional parameters can be divided in four different groups. The first is related to the camera head and optics (parameters of classes 1, 2 and 3). The second group of parameters (Figure 4) is related to the configuration of the camera head and the plane of the turntable (parameters of classes 4 and 5). The third group is related to the turntable itself (parameter of class 6). And finally the fourth group is related to the mechanical errors of the turntable, tumbling, while the camera rotates (parameters of class 7). Tumbling is mainly caused by an incomplete shape of ball bearings and the

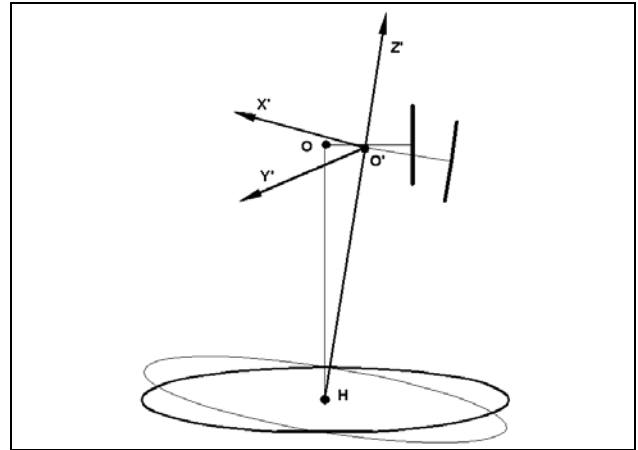


Figure 5. Effect of tumbling: Oscillation of the origin of the auxiliary coordinate system.

contacting surfaces (Matthias, 1961). Tumbling results from the mechanical properties of the instrument. Especially, it is affected by the rotation around the vertical axis and shows its effect as a change of the exterior orientation of the camera head during rotation. From that, one of the main effects of the tumbling is the moving of the origin of the auxiliary coordinate system during rotation (Figure 5). For more detailed information on the mathematical modeling of the tumbling see Amiri Parian and Gruen (2004).

In the next chapter we will report the physical measurement of the tumbling and the result of calibration and accuracy testing with/without the tumbling parameters. We show the results of accuracy tests with minimal number of control points.

## 4. RESULTS

### 4.1. Physical Measurement of the Tumbling

The examination of the tumbling error of the SpheroCam was carried out by an inclinometer. In the present case the Zerotron from Wyler Switzerland is used, which provides the inclination in a specific direction. The inclinometer was placed firmly on the top of the turntable near the gravity center of the camera system. Then using the operating software of the camera, the inclinations of at least 3 continuous rotations ( $1080^\circ$ ) of the turntable at every  $15^\circ$  were recorded. To see

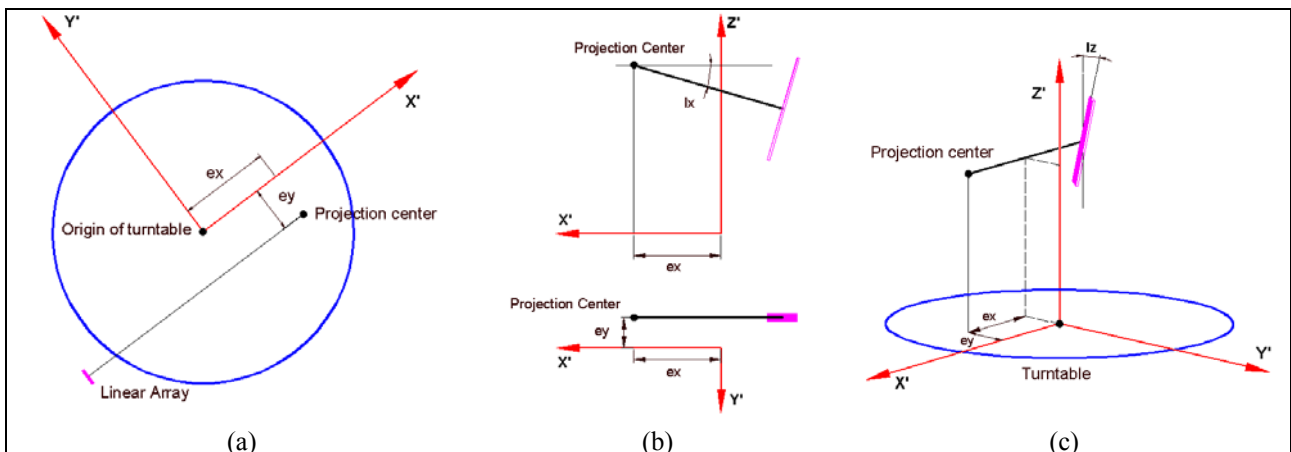


Figure 4. Additional parameters of the configuration of the camera on the turntable. (a) Eccentricity ( $ex, ey$ ), (b) tilt of the linear array ( $lx$ ), (c) inclination of the linear array with respect to the rotation axis ( $lz$ ).

whether the effect is stationary with respect to time, the measurements were carried out at 4 different epochs. Figure 6 shows the observations for one epoch. A Fourier analysis of the signal was carried out, which shows a high peak at the period near  $\pi$  (Figure 6). The analysis of the other epochs shows that the camera is not stable over time. The instability of the camera causes different amplitudes and periods of the observations. Figure 7 shows the observations and the power spectrum of another epoch. These experiences indicate that the camera has a periodic oscillation.

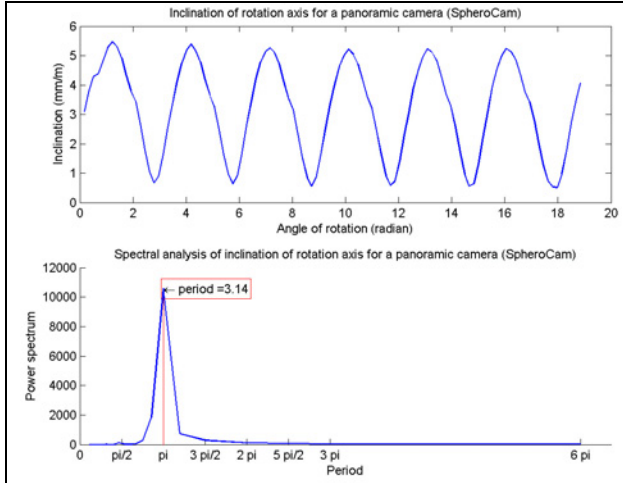


Figure 6. Observations for the inclination of the turntable (top) and the corresponding power spectrum (bottom) for epoch 1.

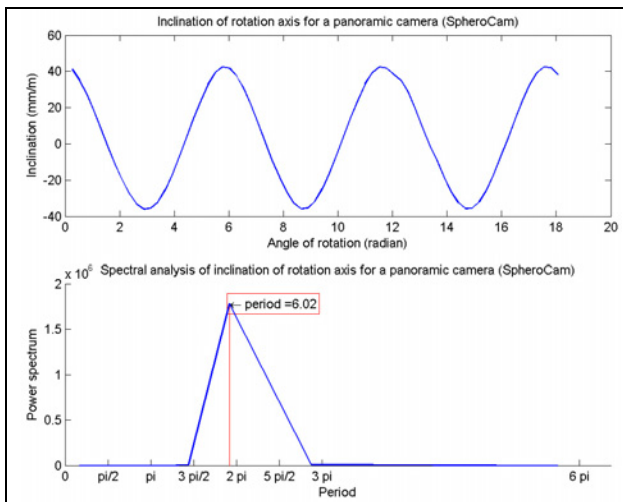


Figure 7. Observations for the inclination of the turntable (top) and the corresponding power spectrum (bottom) for epoch 2.

## 4.2. Camera Calibration

Camera calibration was performed by the mentioned sensor model using additional parameters. For the analysis of the additional parameters (to find the most influential parameters and those which are stable under the given network condition) we added step by step each parameter to the previous stage of the model and used the correlations for stability checking. Comparing the additional parameters of different images, we found the image and block-invariant parameters. We will report the result of calibration in the following sections for the last stage.

### 4.2.1. SpheroCam

The camera calibration was performed using a testfield. We established a testfield with 96 circular targets at our institute and used it for the calibration of the SpheroCam. The testfield was measured with a Theodolite with mean precision of 0.3, 0.3, 0.1 mm for the three coordinate axes (X, Y, Z). The camera calibration was performed by the additional parameters mentioned in chapter 3. To model the tumbling error 6 parameters were used. The a posteriori variance of unit weight is 0.59 pixel (4.7 microns) after self-calibration. Figure 8 shows the residuals of the image point observations in the image space for this case. A comparison of the computed tumbling parameters of different images shows that none of the tumbling parameters is block-invariant. To see the effect of tumbling parameters, a camera calibration was performed with the same condition but without tumbling parameters. In this case the a posteriori variance of unit weight is 1.37 pixels (10.9 microns).

### 4.2.2. EYESCAN

For EYESCAN, we got the image and field observations from Mr. Schneider, TU Dresden. TU's testfield consists of more than 200 control points and the mean precision of control points is 0.2, 0.3, 0.1 mm for the three coordinate axes (X, Y, Z). The camera calibration was performed with the same model and the additional parameters as mentioned in chapter 3. To model the tumbling error of this camera 3 parameters were used. The a posteriori computed variance of unit weight is 0.33 pixel (2.6 microns). Figure 9 shows the residuals of the image point observations in the image space. A comparison of the computed tumbling parameters of different images shows that 2 of 3 tumbling parameters are block-invariant. In the case that tumbling parameters were not used the a posteriori computed variance of unit weight is 1.30 pixels (10.4 microns).

## 4.3. Block Adjustment with Accuracy Test

An accuracy test was performed for EYESCAN by block triangulation using 5 camera stations and by defining 151 check and 3 control points. Considering the result of camera calibration for different images, totally 8 parameters were used as unknown block-invariant, 1 parameter as priori known parameter (camera constant), and 6 parameters as image-invariant parameters. Table 2 shows the summary of the results of adjustment without the modeling of the tumbling. The RMS errors of check points compared with the standard deviations are too large. The reason is that the mathematical model is not complete and cannot interpret the physical behavior of the dynamic camera system. To complete the mathematical model, tumbling parameters were added and the accuracy test was performed. In this case, 8 parameters were used as unknown block-invariant, 4 parameters as a priori known parameters (camera constant and 3 tumbling parameters), and 6 parameters as image-invariant parameters. The summary of the results of adjustment is in the Table 3. Figures 10 and 11 show the object space residuals for checkpoints in depth axes (X and Y) and lateral axis (Z). The RMS errors of check points, compared with standard deviations, are reasonable and shows the effect the tumbling parameters in the modeling. However, the systematic patterns of the residuals have not been completely removed, but the size of the errors is significantly reduced. The remained systematic errors may come from non-modeled mechanical errors of the camera.

For the accuracy test, similar to the conventional close range photogrammetry (frame CDD cameras), 3 control points were

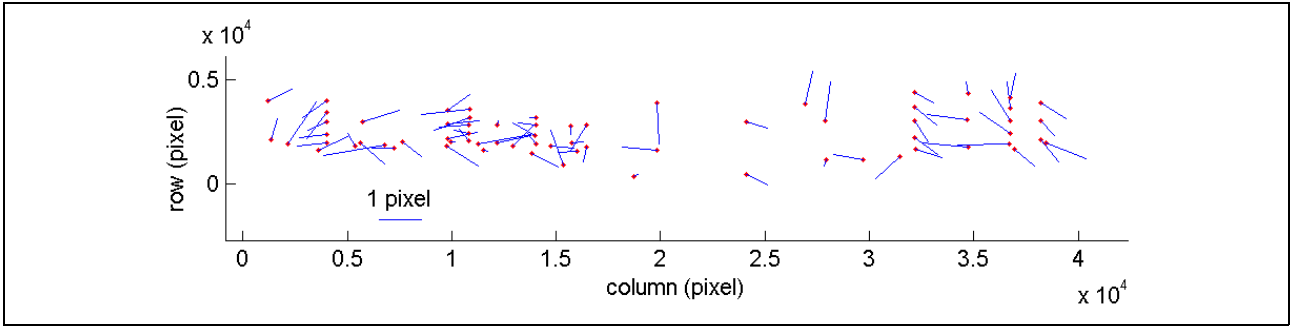


Figure 8. Image space residuals of the observations for the SpheroCam.

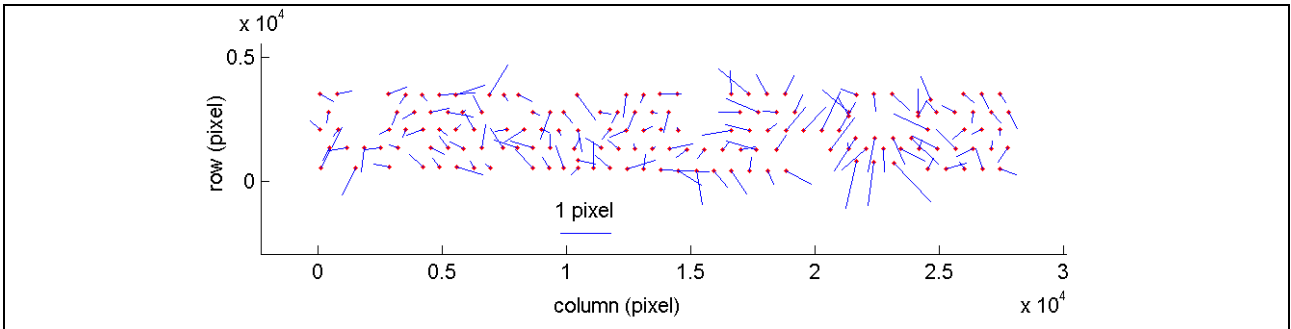


Figure 9. Image space residuals of the observations for the EYESCAN.

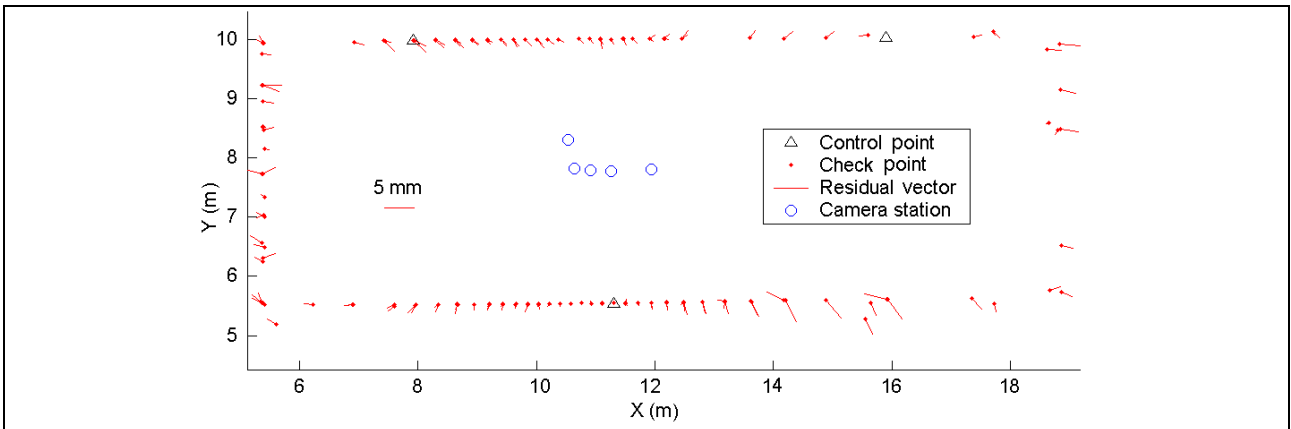


Figure 10. Object space residuals of check points for X and Y axes in XY-plane.

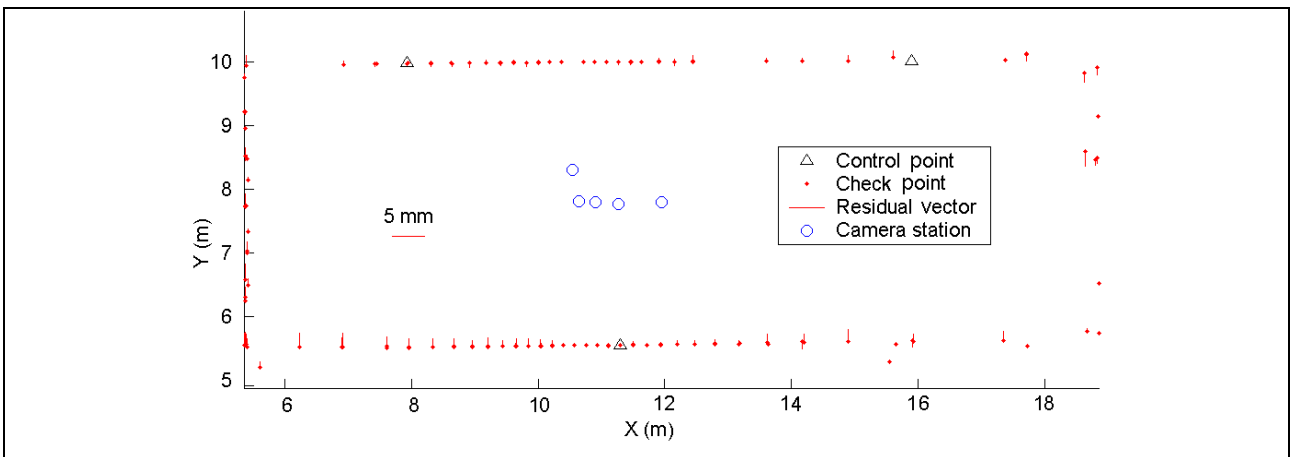


Figure 11. Object space residuals of check points for Z axis in XY-plane.

used to define the datum, since only 6 exterior orientation parameters are datum-dependent. The other parameters were well determined by tie points. However, in the mentioned networks, due to the specific geometry of the camera stations, the camera constant was defined as a priori known parameter to avoid high correlativity of this parameter with check point coordinates. In addition, in the second network tumbling parameters were defined as a priori known parameters since they cannot be determined with a few control points. Although tumbling parameters are not datum-dependent, these parameters model the partial deviations of the orientation parameters of the camera during rotation. Therefore, for a good and reliable estimating, many control points, depending on the number of the tumbling parameters are necessary. We estimated the tumbling parameters of the EYSCAN in the camera calibration process using all control points.

Table 2. Results of accuracy test (without tumbling modeling)

Number of check points	151
Number of control points	3
RMSE of check points (X,Y,Z) (mm)	9.72, 3.72, 3.60
STD of check points (X,Y,Z) (mm)	1.68, 0.64, 0.60
$\hat{\sigma}_0$ (pixel)	0.17 (1.36 microns)

Table 3. Results of accuracy test (with tumbling modeling)

Number of check points	151
Number of control points	3
RMSE of check points (X,Y,Z) (mm)	1.22, 1.04, 0.84
STD of check points (X,Y,Z) (mm)	1.58, 0.60, 0.54
$\hat{\sigma}_0$ (pixel)	0.16 (1.28 microns)

## 5. CONCLUSIONS

We developed an advanced sensor model for panoramic cameras and showed its accuracy performance. We indicated the improvement of the sensor model by the modeling of the tumbling for two terrestrial panoramic cameras EYSCAN and SpheroCam. We measured the tumbling of the SpheroCam using a physical instrument, an inclinometer. The tumbling of the EYSCAN and also the SpheroCam was estimated after bundle adjustment process, in which the tumbling parameters were defined as additional parameters. We performed self-calibration with/without tumbling parameters for EYSCAN and SpheroCam to show the effect of the tumbling modeling. The estimated standard deviations for the observations in image space are 0.59 pixel for the SpheroCam and 0.33 pixel for the EYSCAN in the case of using all mentioned additional parameters, which shows subpixel accuracy for these dynamic systems.

We also investigated the minimal number of control points for determining additional parameters. For the accuracy test 3 control points and 151 checkpoints were used, in which tumbling parameters were considered as a priori known parameters. The achieved accuracy in object space is 1.22, 1.04, 0.84 mm for the three coordinate axes (X, Y, Z) and is reasonable compared to the computed standard deviations. As mentioned before, tumbling parameters were determined in a camera calibration by means of control points. However, other methods should be investigated for determining the tumbling parameters, such as integration of a real time inclinometer or using additional object space information like straight lines, right angles, etc.

The accuracy test with minimal number of control points confirmed that with these new devices we have additional powerful sensors for image recording and efficient 3D modeling. For the near future we plan to investigate further into aspects of network design based on the characteristics of the panoramic cameras and 3D object reconstruction.

## ACKNOWLEDGEMENTS

We appreciate the cooperation of D. Schneider, TU Dresden, who provided us with the image coordinates and control point coordinates for the testing of the EYSCAN camera. We are also grateful to Prof. Dr. L. Hovestadt, ETH Zurich, who rented us his group's SpheroCam for the testfield investigations.

## REFERENCES

- Amiri Parian, J. and Gruen, A., 2003. A Sensor Model for Panoramic Cameras. In Gruen/Kahmen (Eds.), 6th Conference on *Optical 3D Measurement Techniques*, Zurich, Switzerland, Vol. 2, pp. 130-141.
- Amiri Parian, J. and Gruen, A., 2004. A Refined Sensor Model for Panoramic Cameras. International Archives of Photogrammetry, Remote Sensing and Spatial Information Sciences, Vol. XXXIV, part 5/W16. ISPRS "Panoramic Photogrammetry Workshop", Dresden, Germany, 19-22 February 2004.  
[http://www.commission5.isprs.org/wg1/workshop\\_pano/](http://www.commission5.isprs.org/wg1/workshop_pano/)
- Hartley, R., 1993. Photogrammetric Techniques for Panoramic Camera. *SPIE Proceedings*, Vol. 1944, Integrating Photogrammetric Techniques with Scene Analysis and Machine Vision. Orlando, USA, pp. 127-139.
- Matthias, H., 1961. Umfassende Behandlung der Theodolitachsenfehler auf vektorieller Grundlage unter spezieller Berücksichtigung der Taumelfehler der Kippachse. Verlag Leemann, Zürich.
- Scheibe, K., Korsitzky, H., Reulke, R., Scheele, M. and Solbrig, M., 2001. EYSCAN - A High Resolution Digital Panoramic Camera. Robot Vision: *International Workshop RobVis 2001*, Auckland, New Zealand, Volume 1998, pp. 77-83.
- Schneider, D. and Maas, H.-G., 2003. Geometric modeling and calibration of a high resolution panoramic camera. In Gruen/Kahmen (Eds.), 6th Conference on *Optical 3D Measurement Techniques*, Zurich, Switzerland, Vol. 2, pp. 122-129.
- Schneider, D. and Maas, H.-G., 2004. Application of a geometrical model for panoramic image data. International Archives of Photogrammetry, Remote Sensing and Spatial Information Sciences, Vol. XXXIV, part 5/W16. ISPRS "Panoramic Photogrammetry Workshop", Dresden, Germany, 19-22 February 2004.  
[http://www.commission5.isprs.org/wg1/workshop\\_pano/](http://www.commission5.isprs.org/wg1/workshop_pano/)
- Slama, C. C., 1980. *Manual of Photogrammetry*, Fourth edition. American Society for Photogrammetry and Remote Sensing, pp. 196-207.